AD-A163 119 HCL MONITOR PHASE I(U) SPECTRAL SCIENCES INC BURLINGTON MA L S BERNSTEIN ET AL. DEC 85 TR-74 AFESC/ESL-TR-85-25 F08634-84-C-0312 1/1

UNCLASSIFIED F/G 17/5 NL

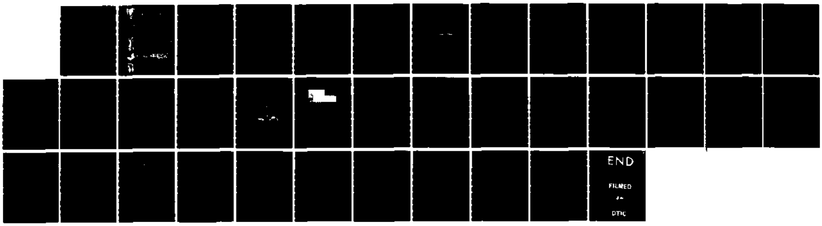

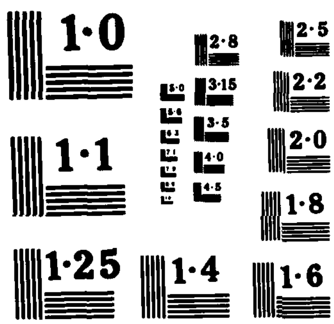

NATIONAL BUREAU OF STANDARDS
MICROCOPY RESOLUTION TEST CHART

1

ESL-TR-85-25

AD-A163 119

HCL Monitor Phase I Final Report

L. S. BERNSTEIN
M. W. MATTHEW
F. BIEN

SPECTRAL SCIENCES, INC.
111 SOUTH BEDFORD STREET
BURLINGTON, MA 01803

DECEMBER 1985

FINAL REPORT

SEPTEMBER 1984 - MAR 1985

APPROVED FOR PUBLIC RELEASE: DISTRIBUTION UNLIMITED

AFESC

AIR FORCE ENGINEERING AND SERVICES CENTER

ENGINEERING & SERVICES LABORATORY
AIR FORCE ENGINEERING & SERVICES CENTER
TYNDALL AIR FORCE BASE, FLORIDA 32403

NOTICE

PLEASE DO NOT REQUEST COPIES OF THIS REPORT FROM HQ AFESC/RD (ENGINEERING AND SERVICES LABORATORY). ADDITIONAL COPIES MAY BE PURCHASED FROM:

NATIONAL TECHNICAL INFORMATION SERVICE
5285 PORT ROYAL ROAD
SPRINGFIELD, VIRGINIA 22161

FEDERAL GOVERNMENT AGENCIES AND THEIR CONTRACTORS REGISTERED WITH DEFENSE TECHNICAL INFORMATION CENTER SHOULD DIRECT REQUESTS FOR COPIES OF THIS REPORT TO:

DEFENSE TECHNICAL INFORMATION CENTER
CAMERON STATION
ALEXANDRIA, VIRGINIA 22314

UNCLASSIFIED

SECURITY CLASSIFICATION OF THIS PAGE (When Data Entered)

REPORT DOCUMENTATION PAGE

READ INSTRUCTIONS BEFORE COMPLETING FORM

1. REPORT NUMBER ESL-TR-85-25	2. GOVT ACCESSION NO. AD-A163 119	3. RECIPIENT'S CATALOG NUMBER
4. TITLE (and Subtitle) HCL Monitor Phase I Final Report		5. TYPE OF REPORT & PERIOD COVERED Final Report 19 SEP 84 to 19 MAR 85
		6. PERFORMING ORG. REPORT NUMBER TR-74
7. AUTHOR(s) L.S. Bernstein, M.W. Matthew, F. Bien		8. CONTRACT OR GRANT NUMBER(s) F08634-84-C-0312
9. PERFORMING ORGANIZATION NAME AND ADDRESS Spectral Sciences, Inc. 111 South Bedford Street Burlington, MA 01803		10. PROGRAM ELEMENT, PROJECT, TASK AREA & WORK UNIT NUMBERS
11. CONTROLLING OFFICE NAME AND ADDRESS HQ AFESC/RDVS Tyndall AFB, FL 32403		12. REPORT DATE December 1985
		13. NUMBER OF PAGES 27
14. MONITORING AGENCY NAME & ADDRESS (if different from Controlling Office)		15. SECURITY CLASS. (of this report) UNCLASSIFIED
		15a. DECLASSIFICATION/DOWNGRADING SCHEDULE

16. DISTRIBUTION STATEMENT (of this Report)

Approved for public release; distribution unlimited.

17. DISTRIBUTION STATEMENT (of the abstract entered in Block 20, if different from Report)

18. SUPPLEMENTARY NOTES

Availability of this report is specified on reverse of front cover.

19. KEY WORDS (Continue on reverse side if necessary and identify by block number)

HCl	Detection	Absorption
Monitor	Infrared	Aerosol
Vapor	White Cell	Space Shuttle
Gas Phase	Emission	

20. ABSTRACT (Continue on reverse side if necessary and identify by block number)

Because of potential environmental effects from the large quantities of HCl released into the atmosphere from Space Shuttle launches it is important to monitor the transport of HCl in both vapor and aerosol form into the surrounding areas. During Phase I of the Air Force 1984-1985 SBIR program, Spectral Sciences, Incorporated investigated the feasibility of developing a man portable HCl monitor capable of unattended operation. The major Phase I objectives were to experimentally demonstrate a novel infrared light (continued)

DD FORM 1 JAN 73 1473 EDITION OF 1 NOV 65 IS OBSOLETE

S/N 0102-LF-014-6601

UNCLASSIFIED

SECURITY CLASSIFICATION OF THIS PAGE (When Data Entered)

20. ABSTRACT (continued)

source and to design an HCl monitor, based on the new infrared source, which would be build and field tested in Phase II. The spectral output of the HCl infrared lamp was measured and was found to be consistent with earlier theoretical predictions. This HCl lamp was used in conjunction with a room temperature HCl absorption cell to demonstrate the potential sensitivity of the approach to measure small ambient HCl concentrations. Even with the relatively crude nature in which the emission-absorption measurements were made, we were able to demonstrate detectable absorption down to 2 ppm for a field instrument. With the improved HCl lamp design and the real time self calibrating optical layout presented in this proposal, we are confident that ambient HCl concentrations as low as 0.1 ppm can be detected with the Phase II instrument.

EXECUTIVE SUMMARY

Because of potential environmental effects from the large quantities of HCl released into the atmosphere from Space Shuttle launches it is important to monitor the transport of HCl in both vapor and aerosol form into the surrounding areas. During Phase I of the Air Force 1984-1985 SBIR program Spectral Sciences, Incorporated investigated the feasibility of developing a man-portable HCl monitor capable of unattended operation. The major Phase I objectives were to experimentally demonstrate a novel infrared light source and to design an HCl monitor, based on the new infrared source, which would be built and field tested in Phase II. The spectral output of the HCl infrared lamp was measured and was found to be consistent with earlier theoretical predictions. This HCl lamp was used in conjunction with a room temperature HCl absorption cell to demonstrate the potential sensitivity of the approach to measure small ambient HCl concentrations. Even with the relatively crude conditions under which the emission-absorption measurements were made we were able to demonstrate detectable absorption down to ~2 ppm for a field instrument. With the improved HCl lamp design and the real time self calibrating optical layout presented in this report we are confident that ambient HCl concentrations as low as 01.1 ppm can be detected with the Phase II instrument.

(The reverse of this page is blank.)

PREFACE

This report was prepared by Spectral Sciences, Incorporated, 111 South Bedford Street, Burlington, MA 01803 under Contract Number F08635-84-C-0312. The work was technically monitored by the Air Force Engineering and Services Center, Engineering and Sevices Laboratory (AFESC/RDVS), Tyndall Air Force Base, Florida, 32403-6001 and funded by the West Coast Office, Air Force Space Technology Center, Box 92960, WPC, Los Angeles, CA 90009-2960.

This report summarizes work accomplished between 19 September 1984 and 19 March 1985. HQ AFESC/RDVS Project Officer was Capt Robert C. Beggs.

This report has been reviewd by the Public Affairs Office (PA) and is releasable to the National Technical Information Service (NTIS). At NTIS, it will be available to the general public, including foreign nationals.

This technical report has been reviewed and is approved for publication.

Robert C Beggs

ROBERT C. BEGGS, Capt, USAF
Project Officer

Robert E. Boyer

ROBERT E. BOYER, Colonel, USAF
Director, Engineering and
Services Laboratory

Robert F. Olfenbuttel

ROBERT F. OLFENBUTTEL, Lt Col, USAF, BSC
Chief, Environics Division

(The reverse of this page is blank.)

TABLE OF CONTENTS

LIST OF FIGURES

LIST OF FIGURES (Concluded)

(The reverse of this page is blank.)

SECTION I

INTRODUCTION

A. NEED TO MONITOR HCl FROM SHUTTLE LAUNCHES

Because of the large quantities of HCl released into the atmosphere from Space Shuttle launches, significant environmental effects are anticipated in the surrounding areas (Reference 1). At present, the short-and long-term environmental effects are not well-quantified, and careful monitoring of the HCl transport into the surrounding areas is required. Previous models and measurements have shown that the amount of HCl deposited on the ground is highly dependent on many local meteorological conditions (temperature, humidity, wind speed and direction, etc) (References 1-11). Furthermore, HCl can persist in both vapor and aerosol forms with the relative partitioning depending upon, among other factors, the HCl and water partial pressures, temperature, and the density and composition of the nucleation sites. Since the concentration and the transport of HCl in the vapor and aerosol forms may be quite different, it is necessary to monitor both forms.

Since many of the proposed monitoring sites are remotely located, a need exists for a portable instrument that can be placed in the field several days prior to a Space Shuttle launch. The HCl monitor must also be capable of unattended operation. Several instruments have been previously developed for monitoring HCl, however they are one-of-a-kind instruments that require expert operators and cannot be simply modified for application to the current problem (References 12-15).

B. NOVEL INFRARED HCl LAMP

During Phase I Spectral Sciences, Incorporated (SSI) has successfully demonstrated a novel approach for monitoring HCl. Our device is based on measuring the infrared absorption of gas-phase HCl and thus makes use of the relatively simple, reliable, and well-developed components of infrared technology. Our technique differs from other infrared approaches (Reference 14) in that we utilize a novel infrared light source. In essence, this source consists of HCl in a heated cell which emits the characteristic HCl line spectrum. The use of a line source matched to its absorption spectrum affords a considerable gain in sensitivity over the use of conventional broadband infrared sources. This allows the use of a more compact multiple-pass absorption cell, which usually is the dominant factor in determining the overall size and complexity of the device. This device can be used to monitor both vapor and aerosol forms of HCl. The vapor HCl is measured directly and the aerosol HCl is determined by preheating the incoming sample in order to vaporize the HCl.

A conceptual view of the advantage of the HCl infrared lamp over a conventional infrared source is shown in Figure 1. Hot HCl emits at characteristic wavelengths, as indicated by the narrow lines. Cold HCl, such as would be found in the atmosphere, absorbs in the same lines as the hot HCl emits. Thus, when the HCl lamp emission is passed through an absorption cell containing HCl, a large decrease in the source intensity is expected. A conventional infrared source, typically a resistively heated piece of metal or ceramic, has a spectrally continuous emission pattern as indicated in Figure 1. When this source is passed through an HCl absorption cell, only a small fraction of the light is absorbed. Detecting HCl absorption with a conventional infrared source then involves measuring a small difference of large signals. With the HCl lamp, however, one is measuring a large difference of large signals.

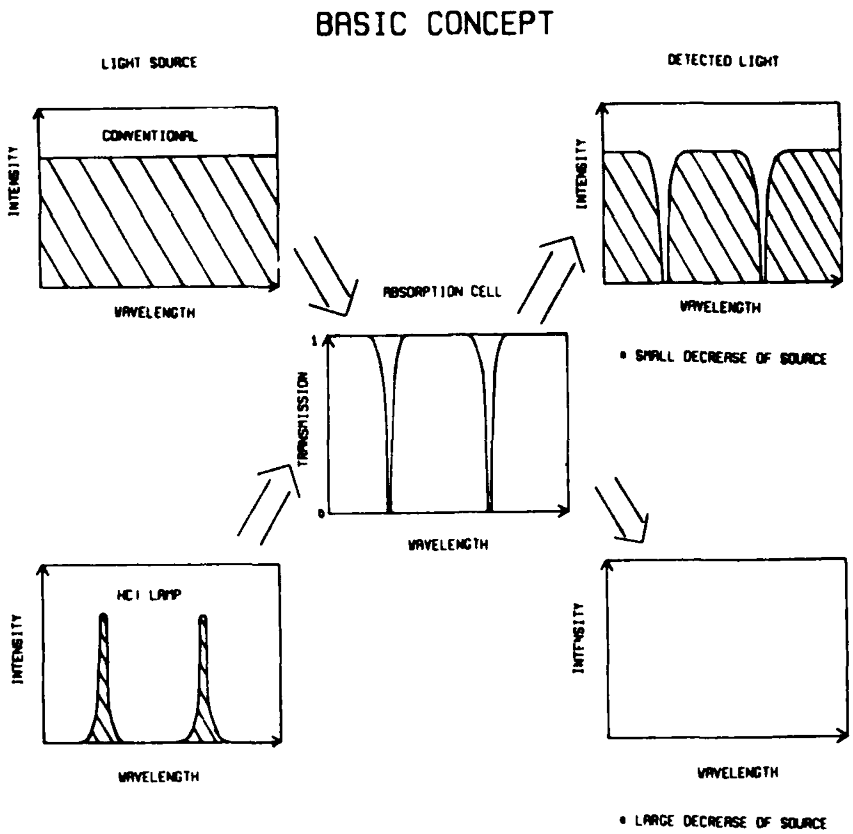

Figure 1. Advantage of HCl Infrared Lamp Over a Conventional Infrared Light Source.

C. PROPERTIES OF HCl EMISSION-ABSORPTION SPECTRUM

The previous section presented a somewhat idealized picture of the HCl emission lamp. In this section, the accurately known spectroscopic parameters (References 16 and 17) of HCl are used to more realistically determine the expected properties of both the HCl emission and absorption spectrum. The well-documented (References 18 and 19) computational algorithms for predicting molecular emission and absorption spectrum are not repeated here.

An example HCl absorption spectrum in the P-branch region is shown in Figure 2. A nearly symmetrical R-branch spectral region exists, although it is not shown, extending from around 2900-3200 cm^{-1}. The designation P or R branch is standard spectroscopic notation for the low- or high-wave number portion of the spectrum of a linear molecular, such as HCl. Within each branch, the individual lines are sequentially numbered (as indicated for the P branch) starting with P(1) and R(0). The lines occur in pairs due to the two isotopic forms of chlorine with natural relative abundances for HCl^{35} of 75.5 percent and for HCl^{37} of 24.5 percent.

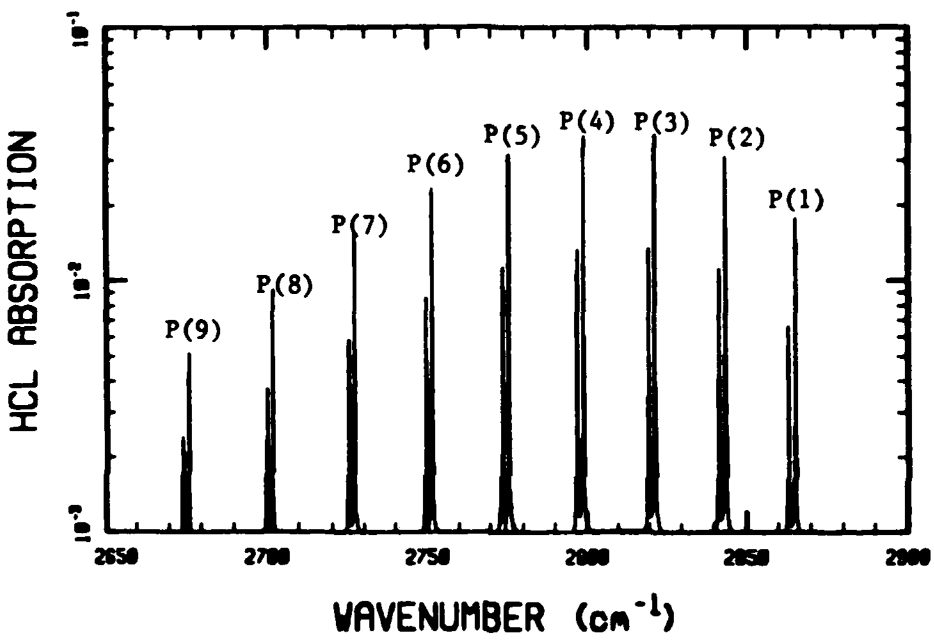

Figure 2. Example HCl Absorption Spectrum. Assumed Conditions: 1 atm Total Pressure, 10 meters Path, 295 K, 0.5 ppm HCl.

An example of the expected HCl lamp emission spectrum is shown in Figure 3. The conditions were chosen so that the peaks of the major isotopic lines ($H^{35}Cl$) are just optically black, and thus reach the indicated blackbody limit. Because the HCl emission occurs at a much higher temperature than the atmospheric absorption, the emission spectrum dies off much slower for the higher rotational lines. This makes it possible to pick one emission line which is strongly absorbed by the cold atmospheric HCl (P(2)-P(5) are possible) and another emission line, P(9) or higher, which is not significantly absorbed by the atmospheric HCl. Similarly, in the R-branch region, the R(1)-R(4) emission lines would be strongly absorbed by atmospheric HCl and the R(9) or higher emission lines would not be significantly absorbed.

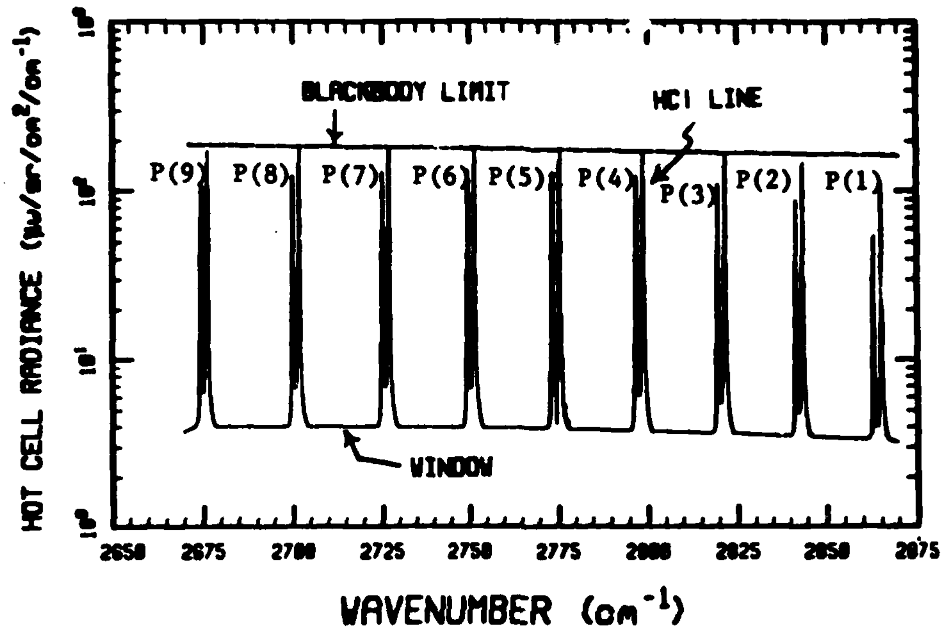

Figure 3. Example HCl Emission Spectrum. Assumed Conditions: 2 cm Path, 800 K, 1.5 atm Total Pressure, 0.15 atm HCl, Sapphire Windows.

The infrared light source is the key element in our measurement scheme. The most significant feature of this source is that the HCl line emission is much higher than the background continuum level from the hot windows. This light source emits most of its energy where HCl absorbs, and small concentrations of HCl in an absorption cell would cause large changes in absorption. The emissions from the windows are minimized by using a very low emissivity material. Both sapphire and water-free quartz are excellent window materials for this application (References 19 and 20). The entire HCl spectrum occurs near the minimum of an atmospheric water vapor transmission window.

D. PHASE I OBJECTIVES

The overall objectives of the Phase I effort were:

- experimental demonstration of the HCl infrared lamp, and

- design of a breadboard HCl monitor to be built and field tested in Phase II

The experimental demonstration of the HCl lamp involved two separate measurements. First, the spectral output of the lamp was measured to ascertain the relative contribution of molecular line emission, window emission and other continuum emission sources. Second, the HCl lamp was used in conjunction with a cold HCl absorption cell to demonstrate the potential sensitivity to the small ambient HCl concentrations expected for the shuttle launches.

The results of the emission and absorption experiments were utilized in the design of the Phase II breadboard monitor. The major considerations in the design effort included optimization of the HCl lamp, selection of emission-absorption measurement spectral bandpasses, and evaluation of material, size, and power constraints. Both the results of the Phase I experiments, as well as the Phase II breadboard monitor design study, are discussed in the following sections.

SECTION II

PHASE I EXPERIMENTS

A. EMISSION EXPERIMENTS

The experimental configuration for the spectroscopic measurements appears in Figure 4. An oven maintained a high temperature (about 700°C at the center) in a 16.3 cm long quartz cell with 1.25 mm thick infrared-quality quartz windows. A CaF_2 lens imaged the radiation from the center of the cell through a chopper and onto the entrance slit of a monochromator (Spex*1681). The smallest slits employed were 0.25 mm, corresponding to 3 wave numbers resolution. A detector (Infrared Industries PbSe type 5757) at the exit slit then provided a signal for a

LAYOUT FOR EMISSION EXPERIMENT

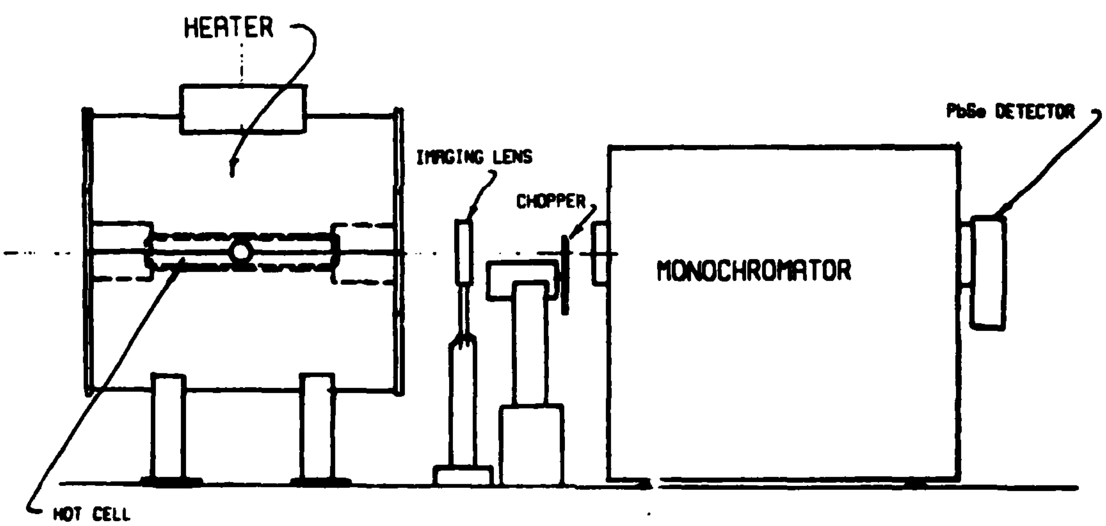

Figure 4. Emission Experiment. Heater Maintains Hot Cell at 700°C. Radiation Passes from Left to Right from Hot Cell, Through Imaging Lens and Chopper, and Falls on Entrance Slit of Monochromator. The Infrared PbSe Detector is at Monochromator Exit Slit.

lock-in amplifier (Princeton Applied Research Model 128A) synchronized to the chopper. The detector was cooled with its attached thermoelectric cooler. The monochromator was scanned through the wavelength region of interest and the emission spectrum was recorded on a strip chart.

Taking a methane spectrum served as a test of the experimental method, since methane is nontoxic and emits in the same region as HCl. The cell held one third of an atmosphere of a mixture of 10 percent methane in nitrogen; the total pressure of this sample rose to one atmosphere at the high temperature, so that the stress on the cell windows was small. A scan several minutes in duration resulted in Figure 5. The individual emission peaks are clearly resolved and correlate well with previous methane absorption spectra.

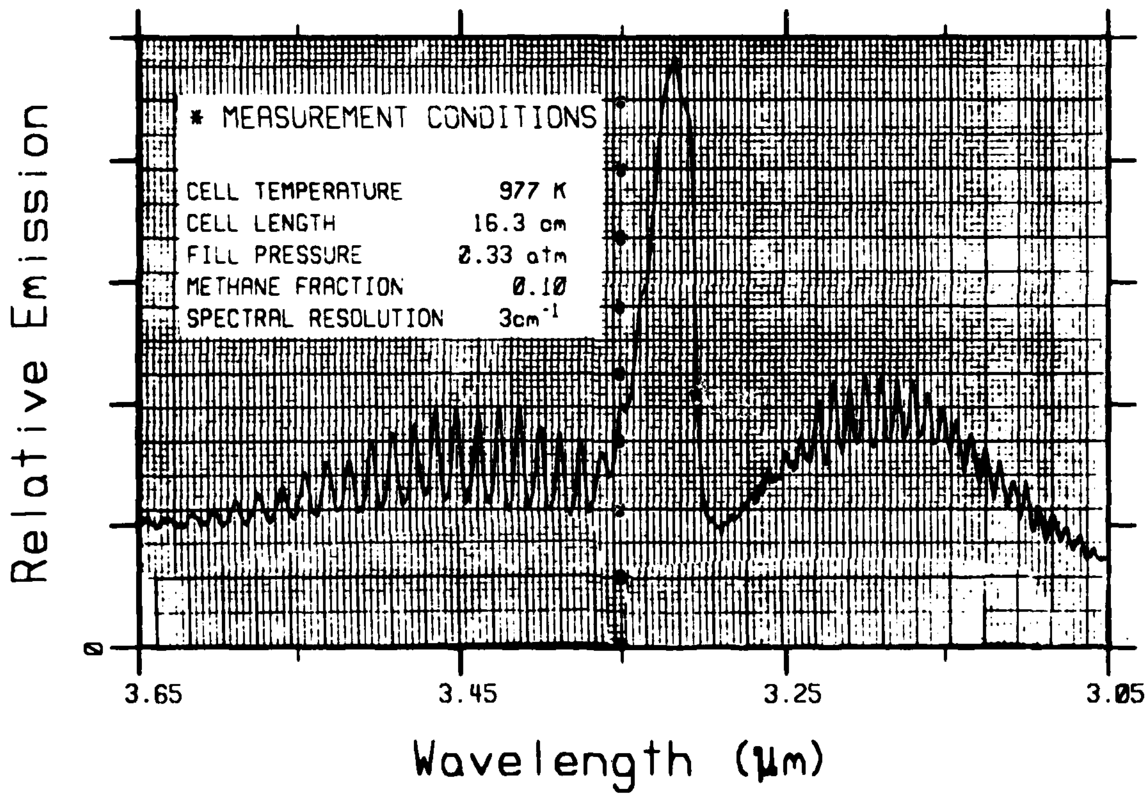

Figure 5. Observed Methane Emission Spectrum.

A representative HCl spectrum appears in Figure 6. The hot cell contained 2 percent HCl in nitrogen, again with the room temperature fill pressure being one-third of an atmosphere.

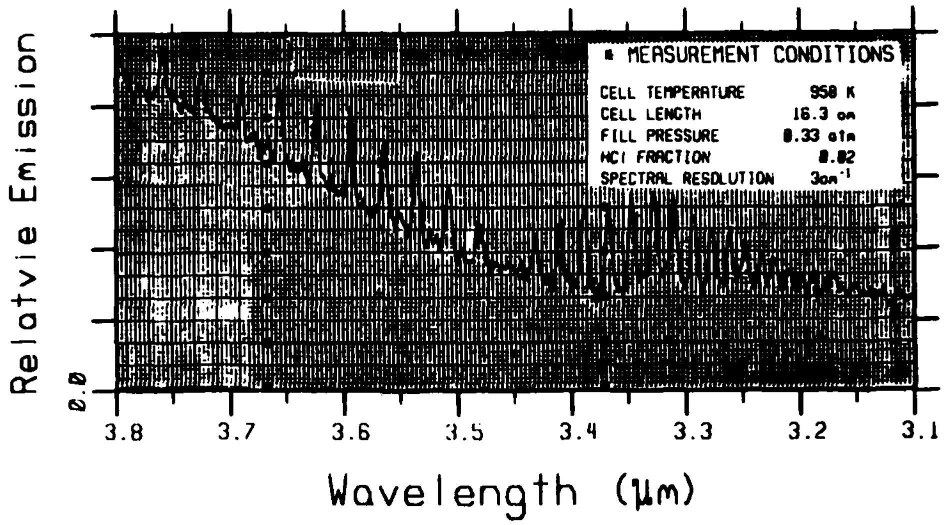

Figure 6. Observed HCl Lamp Emission Spectrum.

1. Analysis of the HCl Emission Spectrum

The emission spectrum of the HCl lamp can be simply modeled in terms of the known optical properties of both the HCl and the quartz windows. The optical parameters which characterize the lamp are the optical opacities (also called optical depth) of the gaseous HCl and the quartz windows. For a gas the optical depth is determined by

$$x = c\,K(\lambda,T,P)\ell \tag{1}$$

where c is concentration, K is the absorption coefficient, and ℓ is path length. The absorption coefficient for a gas generally depends on wavelength, λ, temperature, T, and total pressure, P. The formulas for determining the absorption coefficient for a linear molecular, such as HCl, are well-documented (References 18 and 19) and are not repeated here. For a solid, the optical depth is given by

$$x = K(\lambda,T)t \tag{2}$$

where t is thickness, and the absorption coefficient depends only on wavelength and temperature.

The relative emission (also called emissivity) of the HCl lamp is approximated as a homogeneous source and is given by

$$\epsilon(\lambda) = 1 - \exp(-x_{HCl} - 2x_q) \tag{3}$$

where the factor of $2x_q$ arises because there are two quartz windows. Because the emissivity of quartz is much lower in the P-branch region of the HCl spectrum, we chose this spectral region to perform the absorption sensitivity study which is described in the following section. The emissivity of quartz is nearly flat from around 3 to 3.5 μm. The temperature-dependence of the quartz absorption coefficient is shown in Figure 7.

Using the same conditions as in the measured HCl emission spectrum, the predicted P-branch spectrum is shown in Figure 8. The good agreement with the measured spectrum demonstrates that the behavior of the HCl lamp can be simply and accurately modeled. The relatively high window continuum emission level is due to the rather thick "off-the-shelf" windows which, due to time constraints, had to be used in Phase I. In Phase II, the emission cell will be more compact,allowing thinner windows. We anticipate that the Phase II lamp windows can be about one-third the thickness of the present windows (this is discussed further in Section III). The estimated Phase II lamp output is shown in Figure 9. In this case, the HCl line emission will account for approximately 30 percent of the total light

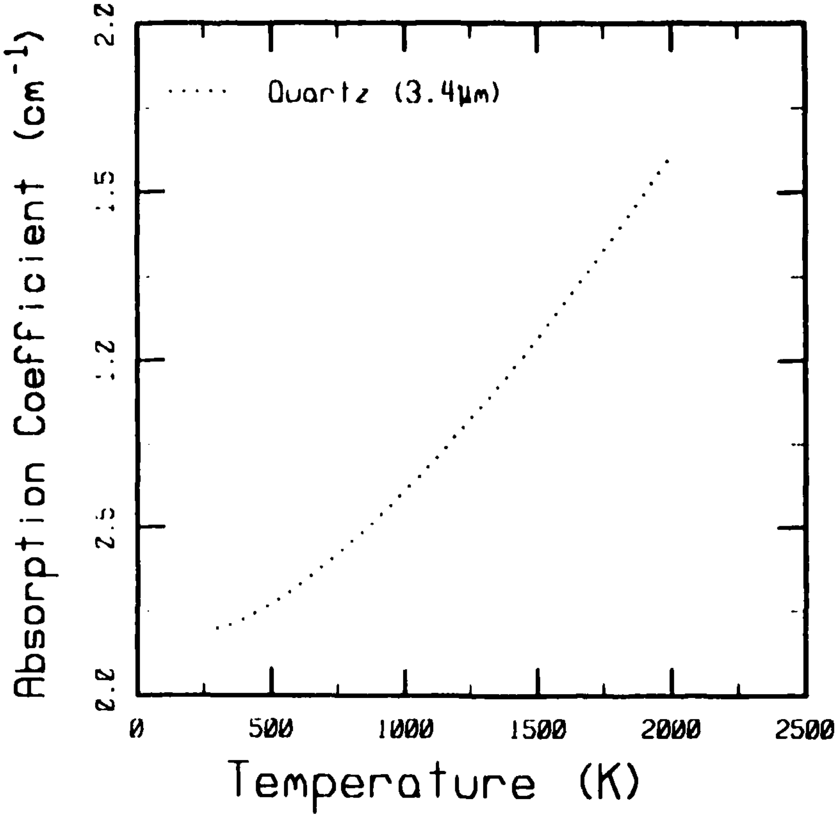

Figure 7. Temperature Dependence of Quartz Absorption Coefficient (Reference 21).

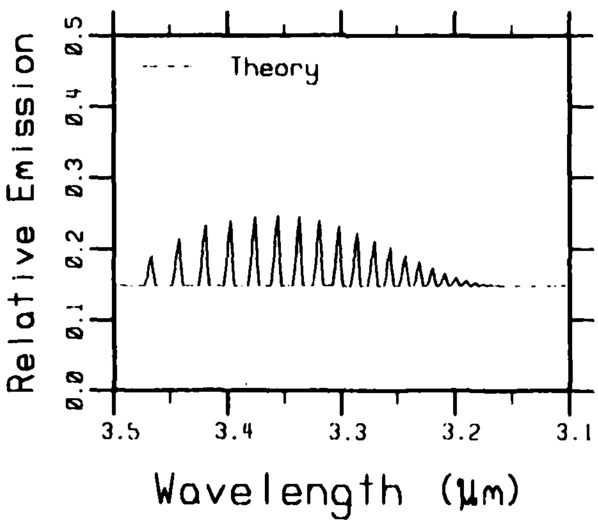

Figure 8. Predicted HCl Lamp Emission Spectrum for Comparison to Observed Spectrum.

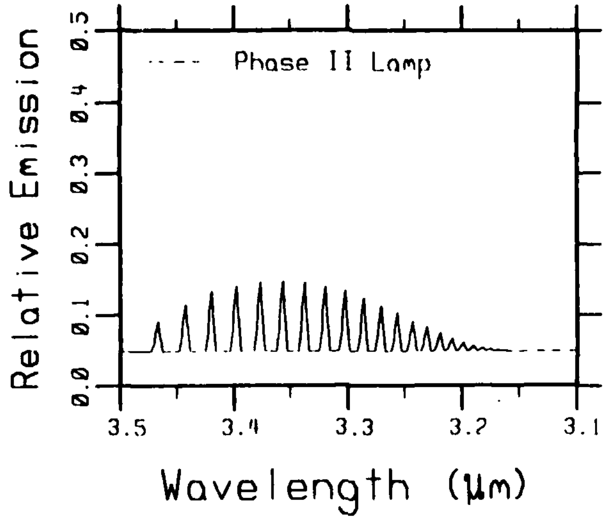

Figure 9. Predicted HCl Lamp Emission Spectrum for Improved Phase II Design.

output. This can be contrasted with a conventional infrared source where only approximately 0.3 percent of the light falls within the HCl absorption lines.

B. ABSORPTION EXPERIMENTS

In these experiments, the image of the center of the hot cell first passed through another cell filled with a room temperature mixture of HCl and nitrogen, and on to a second CaF_2 lens which focussed it directly onto the detector. The arrangement appears schematically in Figure 10. The large detector box was used to situate the small detector at the level of the monochromator exit slit in the emission experiments. The detector and its attendant electronics could otherwise have occupied much less space.

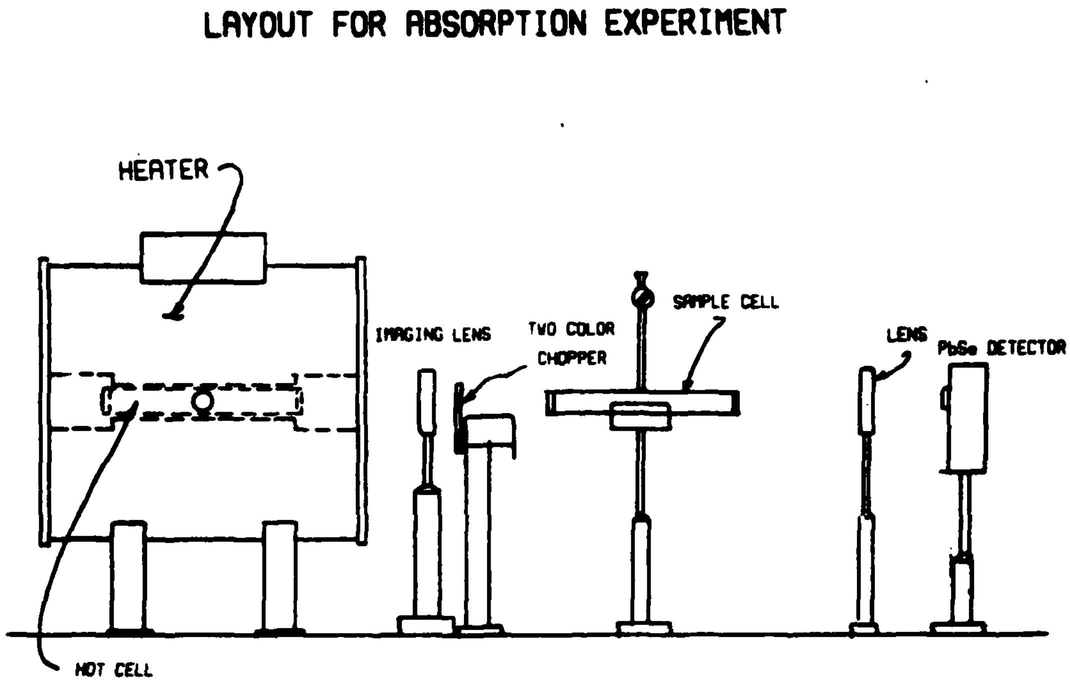

Figure 10. Absorption Experiment. Radiation Passes from Left to Right out of the Hot Cell, Through Imaging Lens and Chopper and is Focussed into Center of Sample Cell. This Image of the Hot Cell is then Imaged by the Second Lens onto the PbSe Detector.

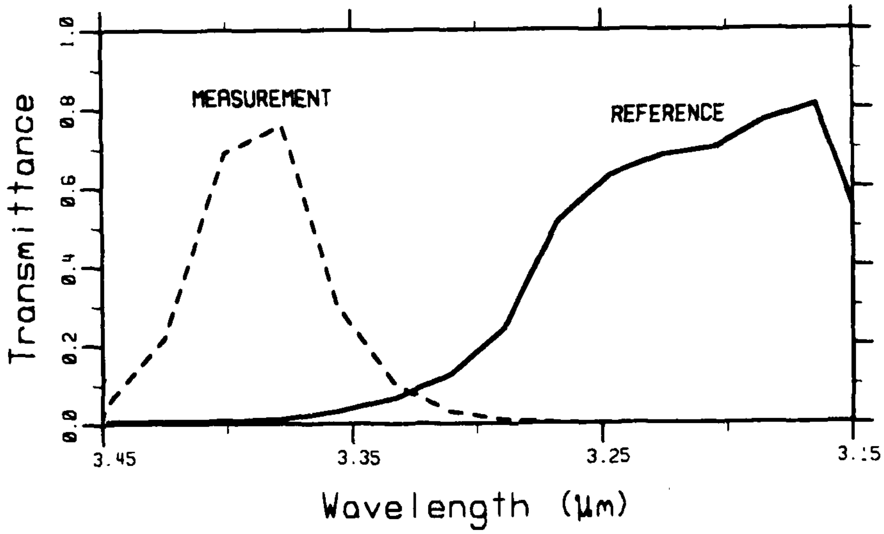

Figure 11. Transmittance Curves for Infrared Filters Used in the Emission-Absorption Measurements.

The chopper immediately followed the first lens. The chopper was a round disk with two off-center holes, 180^{o} apart. Each hole held a bandpass filter; one was centered at 3.2μm, the other at 3.4μm. The filter transmission curves are shown in Figure 11. As discussed below, the room temperature HCl absorbed the emission lines more strongly at the longer wavelength band. Two test tube clamps held the room temperature absorbing cell in the optical path.

The absorptions of several different concentrations of HCl were measured. The output of the detector as a function of time consisted of alternating 3.4 and 3.2μm signal pulses, with intensities I_{abs} and I_{ref} respectively, separated by intervals of no signal. These pulses could either be directly observed on an oscilloscope or directed to an A/D converter linked to a computer (Compaq) for measurement. Both measurement techniques gave consistent results. All the plotted data came from the computer, which was preferred for its ease of use and precision. The ratio of the absorbing to the nonabsorbing band intensities for the cell containing HCl,

$$R_1 = \frac{I_{abs}}{I_{ref}} \quad , \tag{4}$$

is one of the two ratios needed for calculation of the HCl concentration. The other required ratio is that of these two bands for a path containing no HCl, in order to normalize R_1 to the total intensities in each band. Here, the intensities are called I^{o}_{abs} and I^{o}_{ref}, and their ratio is

$$R_2 = \frac{I^{o}_{abs}}{I^{o}_{ref}} \quad . \tag{5}$$

A breadboard instrument will include both paths in its optical design. Replacing the HCl-containing cell with an empty cell provided a simulation of such an arrangement for these experiments. Here, however, the measurements of the two ratios occurred about a minute apart, while the breadboard instrument will make both measurements once per chopper rotation, within a fraction of a second. For the present results, small drifts in the detector response and the emission cell temperature occurred between the two measurements and contributed to the scatter of the data. The test tube clamps did not allow highly reproducible positioning of the absorbing and empty cells, so that, in some cases, some radiation from the hot cell walls might have been reflected by the wall of the second cell into the detector, increasing the background over the molecular emission.

The concentration of HCl is correlated with the absolute transmittance τ, where

$$\tau = R_1/R_2 \quad . \tag{6}$$

This overall ratio is slightly less than 1.0, which is its limiting value as the concentration approaches zero. The difference between the overall ratio and 1.0, the fractional absorption

$$\alpha = 1 - \tau \quad , \tag{7}$$

thus, increases with concentration. Figure 12 contains the measured values of α plotted against concentration. Each measurement is the average of a number of values of α. The error bars show the root mean square deviation of the measurements. The actual HCL concentrations in one atmosphere of mixture in the absorbing cell were 132 ppm, 316 ppm, 1147 ppm, and 2240 ppm. However, the absorption is proportional to the product of concentration and path length, so the concentrations shown in the figure are reduced from the experimental values by the ratio of the 16.3 cm path length in the present experiment to the 10-meter path length in the proposed breadboard instrument. The concentrations in the plot then match the concentrations which would produce the observed overall ratios in the breadboard. Despite the inaccuracies with the present preliminary measurement technique, concentrations down to 2 ppm provided clearly detectable changes in the average overall ratio.

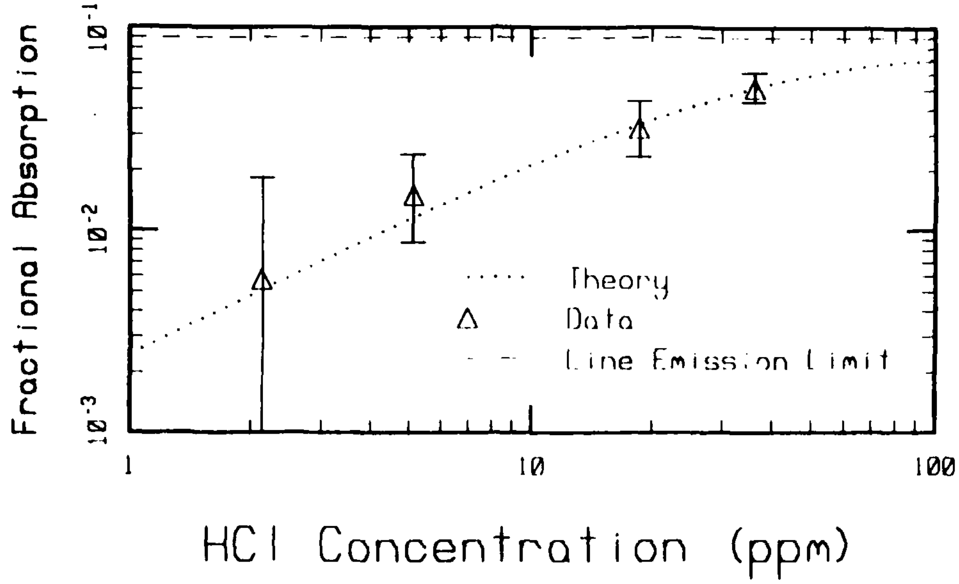

Figure 12. **Comparison of Measured to Predicted Fractional Absorption of HCl Emission Lamp by HCl Absorption Cell.** (Calculated concentrations based on a 10-meter pathlength)

1. **Analysis of Emission-Absorption Experiment**

The dependence of the fractional absorption of light on the concentration of HCl in the absorption cell is modeled by

$$\alpha = 1 - \frac{I_1}{I_0} \quad , \tag{8}$$

where

$$I_1 = \int \epsilon(\lambda)\ \tau_a(\lambda)\ \tau_f(\lambda)\ d\lambda \tag{9}$$

$$I_0 = \int \epsilon(\lambda)\ \tau_f(\lambda)\ d\lambda \tag{10}$$

where $\epsilon(\lambda)$ is the emissivity of the HCl lamp, $\tau_a(\lambda)$ is the transmission function of the HCl in the absorption cell, and $\tau_f(\lambda)$ is the infrared filter transmission function. The comparison of the theoretical to the observed fractional absorption is shown in Figure 12. Note that the experimental results are presented in terms of an equivalent concentration for a 10 meter absorption path. The 10 meter path length will be used in the Phase II breadboard by employing a multiple-reflection 40-pass white cell of length 25 cm. The good agreement between the theoretical and experimental results demonstrates that the basic measurement concept is sound. In spite of the crude nature in which the emission-absorption experiments were performed it is remarkable that we were able to demonstrate a detectable absorption as low as ~2 ppm. With the improved emission cell design and the real-time self-calibrating optical layout discussed in Section III, we are confident that an ambient HCl concentration as low as 0.1 ppm should be readily detectable with the Phase II instrument.

SECTION III

PHASE II BREADBOARD HCl MONITOR

This section describes the breadboard instrument to be constructed in Phase II. The instrument consists of a specially designed HCl infrared lamp source, which goes through a long-path absorption cell whose optical train and operation are discussed in Section IIIA. The description of the source is discussed in Section IIIB.

The portable breadboard instrument would feature this optical arrangement, mounted so that both calibration and field testing can be achieved, and would include a means for cycling new air, which may contain HCl in either vapor or aerosol forms, through the instrument. From this breadboard instrument, a ruggedized field instrument design can be finalized.

A. OPTICAL TRAIN

The optical train of the proposed instrument is shown in Figure 13. Phase II of this program would involve construction of a breadboard apparatus using this arrangement and carrying it from laboratory proof of principle, through calibration, to field testing. The breadboard instrument could be modified in the development of a brassboard prototype for Phase III.

The optical train is centered on a HCl lamp (1) which is described in more detail in Part B of this section. Light from this lamp is focused through lens (2) and directed by mirrors (3) and (4) into a long-path absorption cell. Some of the light is split off from this beam by a beam splitter (5) to form a reference leg. The light is also chopped by a filter wheel (6) so that it passes two colors, alternately, into the long path absorption cell.

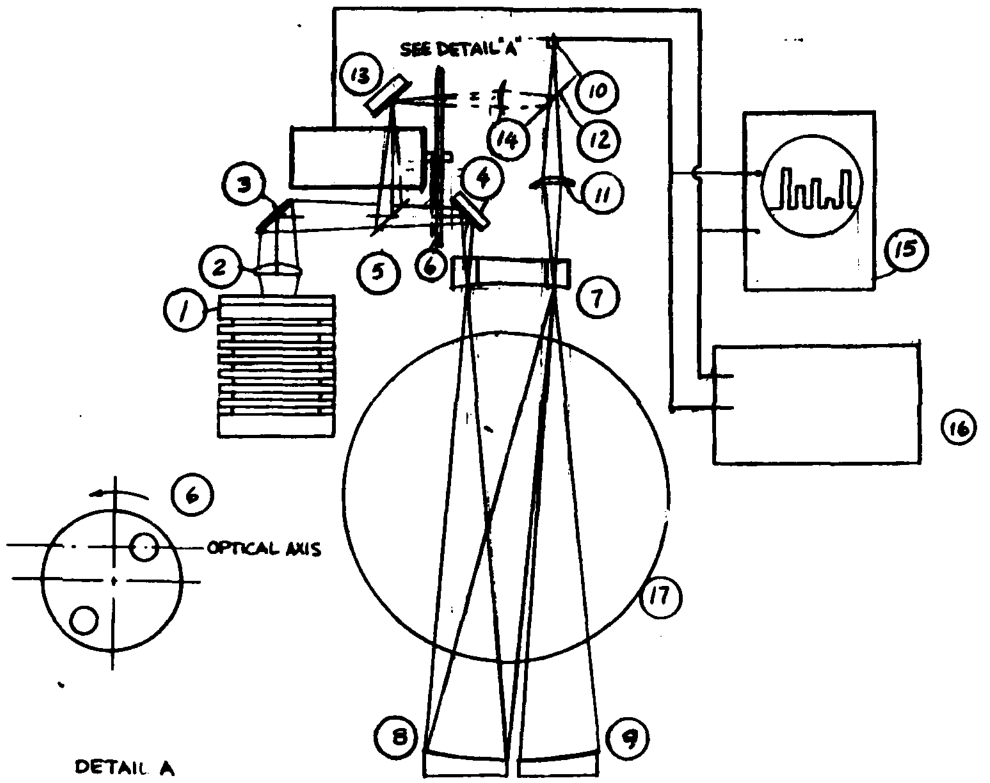

Figure 13. Optical Layout for Phase II Breadboard Instrument. See Subsection IIIA for Detailed Description of Each Numbered Part.

The long-path absorption cell is of a white-cell geometry, with a numerical aperture of F:6 and a pathlength of 25 cm (10 inches). Using multiple passes, a total path of 10 meters forms the absorption region. The multiple pass cell consists of three mirrors (7), (8) and (9) each having a radius of curvature equal to 25 cm and separated by 25 cm, as shown in Figure 13. The light focused through a slot cut in the front mirror (7) is reflected by mirror (8) and refocused onto mirror (7). Because of the curvature on mirror (7), light is reflected onto mirror (9), which again returns the light to mirror (7) only at a new location. After a total of

40 passes, or 19 reflections on mirror (7) and 10 reflections on each mirror (8) and (9), the light leaves the cell through a second slot on mirror (7). This light is an expanding cone which is refocused onto the detector (10) by lens (11). A beam splitter (12) directs the radiation coming via the reference leg so that it also falls on the detector (10).

The reference leg consists of a mirror (13) and a lens (14) which brings this light to focus onto the detector when the filter wheel is in the pass position. The light from the HCl emission source is thus, alternately brought through the reference leg and the sample call. By placing the filter wheel out of the plane of Figure 13 such that the chopper passes light when the filter is at a 45-degree angle (see Detail A) light would come through the chopper such that the reference beam leads the signal beam by 90 degrees.

The filter wheel is fitted with two circular filters, as shown in Detail A. Light passes through one filter which provides a reference wavelength where HCl does not absorb, and a second filter where the HCl does absorb. The drift, due to detector sensitivity and lamp temperature variations, is monitored by light passing through the reference path. A simulated signal is illustrated on the oscilloscope (15). This signal consists of the reference signal from the reference filter at zero degrees rotation of the wheel followed by 90^{o} in the rotation of the filter wheel, the reference signal through the long path absorption cell, followed at 180^{o} by the absorption band filter through the reference path, and finally at 270^{o} the absorption filter through the absorption path. The signal and reference position of the filter wheel are entered together into a demodulating circuit (16) which, in turn, outputs the total amount of HCl in the absorption path.

The instrument thus, draws air through the absorption path, represented by the circle (17), fills the region between mirrors (7) and (8) plus (9), and monitors this air for HCl content. To measure both the aerosol and gaseous HCl, the air may be preheated to evaporate aerosols and break up hydrates before they enter the absorption path. The total size of this flow instrument, together with the optical train and monitoring equipment, is on the order of 1 to 2 ft^3. The optical train itself could be built with a maximum dimension of 0.5 meters (20 inches).

B. HCl LAMP OPTIMIZATION

As discussed in the previous section, the laboratory portion of Phase I demonstrated the feasibility of using an HCl emission source to illuminate an atmosphere which contains trace quantities of HCl. The laboratory HCl lamp was constructed from "supersil" quartz and put into a commercial oven. The size of the Phase I lamp, its suspension method, its emission solid angle, and its orientation were all more fixed by the use of the commercial oven rather than by any fundamental physical or optical constraints.

The development of a tailored lamp is discussed here. The size, aperture, and power requirements for an operational system are analyzed for a proposed prototype design. Other design constraints, such as mounting requirements and baffle design, would be left until after the breadboard HCl detector has been tested, as these parameters are somewhat driven by the operational characteristics of the instrument.

The design of the brassboard lamp is shown in Figure 14. This lamp consists of a quartz cell with optically flat windows (1) which is filled to 1/3 atm of a N_2, HCl mixture, then sealed. The dimensions of this cell are approximately 4 mm diameter and 2.54 cm long. The window thickness of 0.5 mm (.02 inches) minimizes window emissivity while providing adequate structural strength. The cell is supported in an oven by a high temperature ceramic potting compound (2) in which is embedded 24 ga. Kanthal wire (Fe-Cr-Al-Co alloy) (3). The kanthal wire passes through the side of the beater assembly (4) by ceramic feed-throughs (5). The kanthal wire is heated resistively by passing current from either a battery or a small generator in the breadboard instrument.

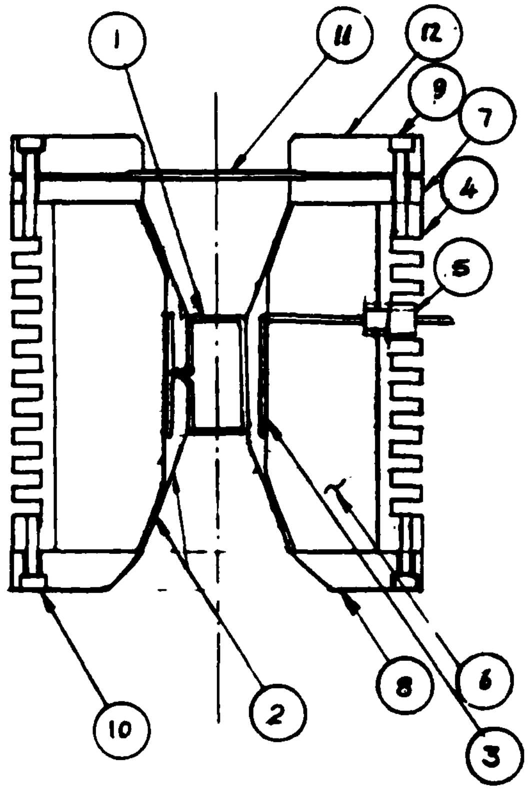

Figure 14. Phase II HCl Lamp Design. See Subsection IIIB for Detailed Description of Each Numbered Part.

To minimize the heat loss of the lamp, approximately 1-inch thick ceramic fiber insulation (6) shields the heater wire from the outside body. The top and bottom of the heater assembly uses end bells (7) and (8) to contain this insulation. These are attached by small screws (9) and (10) along the perimeter of the heater. To further reduce heat loss, a sapphire window (11) is placed on the front (top) side of the heater and held in place with retainer (12). The entire housing of this lamp is made of black anodized aluminum to keep the outer jacket from becoming too hot.

The main sources of energy loss, other than the radiation in the HCl band, are due to black body radiative losses near the heater coils, conduction through the ceramic, and convection of heat from the hot parts to the end window, a subsequent conduction to the heater frame. The outer metal jacket is designed to lose heat efficiently to the surrounding air, so that the lamp can operate at a constant temperature.

The energy consumed due to radiation losses is given by

$$Q_R = A\epsilon\sigma T^4 \tag{11}$$

where A is the radiating surface area, ϵ the emissivity equal to 0.8 for the portions of the insulation doing the radiating, σ the Stefan-Boltzmann constant is equal to $5.7 \times 10^{-12} W/^{o}K^4 cm^2$, and T is the temperature, picked at a conservative 1000 ^{o}K. The surface area is approximately 6 cm^2 for the exposed portions of the cell. Thus, the radiative loss is approximately 27 watts.

Conduction through the side walls which directs heat away from the cell region is minimized by using a ceramic paper insulation. This insulation has conductivities ranging from 0.3 to 0.5 Btu in/hr ft^2 ^{o}F, corresponding to $k=5$ to 7×10^{-4} $W/cm^{o}K$. The conduction heat-loss equation is given by:

$$Q_C = \frac{2\pi k \ell \Delta T}{\ln(r_o/r_i)} \tag{12}$$

where r_o is the outer radius of the insulation, equal to 3.5 cm, r_i is the inner radius, equal to 1 cm, and L is the length of the cell, equal to 7.5 cm. The temperature drop across the insulation is approximately 650 to $700^{o}K$. Thus, Q_C = 17 watts.

The convective heat losses of the lamp are much harder to estimate, but by assuming worst-case conditions, that of free convection across the hot windows transferring energy to the sapphire flats, Nusselt numbers of approximately

$$Nu_x = \frac{hx}{k} = 0.38 \tag{13}$$

are expected, where h is the convective heat transfer coefficient in watts/cm^2 ^oK, K is the conductivity of air, equal to 6.5×10^{-4} Watts/cm ^oK, and x is the boundary layer thickness, $\simeq$ 1 cm. Thus, $h = 2.4 \times 10^{-4}$ watts/cm^{2o}K, and the total heat loss through convection is on the order of 1 watt. Thus, for the design shown in Figure 14, the total power dissipation is on the order of 45 watts, the major portion of which is due to radiation through the end ports.

The lamp design shown in Figure 14 has several unique features. The lamp is arranged vertically so that free convection does not cool down the cell windows. The sapphire flat on the top end forms a "storm window" effect to minimize convective heat losses. High-resistivity insulation is used to minimize conductive losses through the side walls. Finally, a minimum exposed area has been designed into the lamp to minimize radiative losses and still provide an acceptable aperture (lamp solid angle).

This lamp design would be constructed in the Phase II development portion of the contract and tested to assure proper operation.

REFERENCES

1. Potter, A.E., "Environmental Effects of the Space Shuttle," J. Environmental Sciences, 21, 15 (1978).

2. Sebacher, D.I., Bendura, R.J., and Gregory, G.L., "Hydrogen Chloride Measurements in the Space Shuttle Exhaust Cloud - First Launch, April 12, 1981," J. Spacecraft & Rockets, 19, 366 (1982).

3. Fenton, D.L. and Ranade, M.B., "Aerosol Formation Threshold for HCl-Water Vapor System," Environmental Science & Technology, 10, 1160 (1982).

4. Knuston, E.O., Fenton, D.C., Walanski, K., and Stockham, J.D., "Washout Coefficients for Scavenging of Rocket Exhaust HCl by Rain," Sixth Conference on Aerospace and Aeronautical Meteorology, American Meteorological Society, El Passo, Texas (1974).

5. Rhein, R.A., "Hydrochloric Acid Aerosol Formation by the Interaction of HCl with Humid Air," JPL TM-33-658 (1973).

6. Sebacher, D.I., Wornom, D.E., and Bendura, R.J., "Hydrogen Chloride Partitioning in a Titan III Exhaust Cloud Diluted with Ambient Air," AIAA Paper 79-0299 (1980).

7. Sebacher, D.I., Bendura, R.J., and Wornom, D.E., "Hydrochloric Acid Aerosol and Gaseous Hydrogen Chloride Partitioning in a Cloud Contaminated by Solid Rocket Exhaust," Atmospheric Environment, 14, 543 (1980).

8. Pellett, G.L., "Analytic Model for Washout of HCl(g) From Dispersing Rocket Exhaust Clouds," NASA TP-1801, (1981).

9. Anderson, B.J. and Keller, V.W., "Space Shuttle Exhaust Cloud Properties," NASA TP-2258, Marshall Space Flight Center, Alabama, (1983).

10. Gregory, G.L., Woods, D.C., and Sebacher, D.I., "Airborne Measurements of Launch Vehicle Effluent-Launch of Space Shuttle (STS-1) on April 12, 1981," NASA TP-2090, NASA Langley Research Center, Hampton, Virginia (1983).

11. Maddrea G.L., Jr., Gregory, G.L., Sebacher, D.I., and Woods, D.C., "Airborne Measurements of Launch Vehicle Effluent of STS-2 Launch on November 12, 1981, at Cape Canaveral, Florida," NASA TP-2260, NASA Langley Research Center, Hampton, Virginia (1984).

12. Wornom, D.E., Woods, D.C., Thomas, M.E., and Tyson, R.W., "Instrumentation of Sampling Aircraft for Measurement of Launch Vehicle Effluents," NASA TM X-3500, (1977).

13. Gregory, G.L. and Moyer, R.H., "Evaluation of Hydrogen Chloride Detector for Environmental Monitoring," Rev. Sci. Instruments, 48, 1464 (1977).

14. Sebacher, D.I., "Airborne Nondispersive Infrared Monitor for Atmospheric Trace Gases," Rev. Sci. Instruments, 49, 1520 (1978).

15. Cofer, W.R. and Pellett, G.L., "Absorption and Chemical Reaction of Gaseous Mixtures of Hydrogen Chloride and Water on Aluminum Oxide and Application to Solid-Propellant Rocket Exhaust Clouds," NASA TP-1105, (1978).

16. Rothman, L.S., Goldman, A., Gilles, J.R., Tipping, R.H., Brown, L.R., Margolis, J.S., Maki, A.G., and Young, L.D.G., "AFGL Trace Gas Compilation: 1980 Version," Appl. Opt., 20, 1323 (1981).

17. McClatchey, R.A. and Selby, J.E.A., "Atmospheric Attenuation of Laser Radiation From 0.76 to 31.25 μm," AFCRL-TR-74-0003, Air Force Geophysics Laboratory, Hanscom Field, Bedford, Massachusetts (1974).

18 Ludwig, C.B., Malkmus, W., Reardon, J.E., and Thomson, J.A.L., "Handbook of Infrared Radiation from Combustion Gases," NASA SP-3080, (1973).

19. Wolfe, W.L. and Zissis, G.Z., (ed.), "The Infrared Handbook," Office of Naval Research, Department of the Navy, Arlington, Virginia, (1978).

20. Amersil, Inc., "Optical Fused Quartz and Fused Silica," 650 Jerners Mill Road, Sayreville, New Jersey 08872.

21. Beder, E.C., Bass, C.D., and Shackleford, W.L., "Transmissivity and Absorption of Fused Quartz Between 0.22 μ and 3.5 μ from Room Temperature to 1500°C", Appl. Opt., 10, 2263 (1971).

(The reverse of this page is blank.)

END

FILMED

2-86

DTIC